

Prone Position for Preoperative Planning in Lumbar Endoscopic and Minimally Invasive Fusion Procedures: Insights From a Magnetic Resonance Imaging Study

Miguel Relvas-Silva, José Maria Matos Sousa, Daniel Dias, Bernardo Sousa Pinto, António Sousa, José Fonseca, Miguel Loureiro, André Rodrigues Pinho, Vitorino Veludo, António Serdoura, Maria Dulce Madeira and Pedro Alberto Pereira

Int J Spine Surg published online 2 April 2025
<https://www.ijssurgery.com/content/early/2025/04/01/8731>

This information is current as of April 4, 2025.

Email Alerts Receive free email-alerts when new articles cite this article. Sign up at:
<http://ijssurgery.com/alerts>

Prone Position for Preoperative Planning in Lumbar Endoscopic and Minimally Invasive Fusion Procedures: Insights From a Magnetic Resonance Imaging Study

MIGUEL RELVAS-SILVA, MD^{1,2,3,4}; JOSÉ MARIA MATOS SOUSA, MD⁵; DANIEL DIAS, MD¹;
BERNARDO SOUSA PINTO, MD, PhD^{6,7}; ANTÓNIO SOUSA, MD, PhD¹; JOSÉ FONSECA, MD⁵;
MIGUEL LOUREIRO, MD^{1,8}; ANDRÉ RODRIGUES PINHO, MD, PhD^{1,3,4,9}; VITORINO VELUDO, MD¹;
ANTÓNIO SERDOURA, MD¹; MARIA DULCE MADEIRA, MD, PhD^{3,4,9}; AND PEDRO ALBERTO PEREIRA, PhD^{3,4,9}

¹Department of Orthopedics and Traumatology, ULS São João, Porto, Portugal; ²Department of Surgery and Physiology, Faculty of Medicine, University of Porto, Alameda Professor Hernâni Monteiro, Porto, Portugal; ³Unit of Anatomy, Department of Biomedicine, Faculty of Medicine, University of Porto, Alameda Professor Hernâni Monteiro, Porto, Portugal; ⁴NeuroGen Research Group, Center for Health Technology and Services Research (CINTESIS), Rua Dr. Plácido da Costa, Porto, Portugal; ⁵Department of Neuroradiology, ULS São João, Porto, Portugal; ⁶MEDCIDS—Department of Community Medicine, Information and Health Decision Sciences; Faculty of Medicine, University of Porto, Porto, Portugal; ⁷CINTESIS@RISE—Health Research Network, MEDCIDS, Faculty of Medicine, University of Porto, Porto, Portugal; ⁸Hospital das Forças Armadas, Porto, Portugal; ⁹CINTESIS@RISE, Faculty of Medicine, University of Porto, Alameda Professor Hernâni Monteiro, Porto, Portugal

 MR-S, 0000-0003-1018-0810;  JMMS, 0000-0002-1277-3401;  DD, 0000-0002-0951-8872;  BSP, 0000-0002-1277-3401;  AS, 0000-0002-4140-6694;  ML, 0009-0005-5911-7611;  ARP, 0000-0003-1277-0638;  VV, 0000-0003-2093-3679;  MDM, 0000-0002-0721-6547;  PAP, 0000-0003-2298-3143

ABSTRACT

Background: Differences in lumbar morphology and nerve root positioning between supine and prone decubitus are poorly analyzed. This study aimed to perform a magnetic resonance imaging (MRI) study to describe lumbar morphology, nerve root, and related structures positioning in the prone position, while comparing with conventional supine MRI, in patients with lumbar symptoms. The second aim was to define safe working zones for lumbar surgical procedures.

Methods: This study was a prospective, single-center, observational study. Fifty patients with persistent low back and/or radicular pain that was unresponsive to conservative treatment were consecutively selected. Supine and prone 3 Tesla MRIs were performed. Two independent researchers performed an imaging analysis of predefined variables.

Results: Lumbar lordosis significantly changed from 49.3° in the supine position to 52.1° in the prone position ($P = 0.005$), without a statistically significant difference in lower lumbar lordosis. No consistent changes were found regarding foraminal height, root-to-pedicle or root-to-superior articular process distances. The exiting nerve root was found between 42% and 49% of the foraminal height (as measured from the upper border of the lower pedicle). The left retroperitoneal lateral corridor showed no significant size variation from the supine to the prone position ($P = 0.196$ and $P = 0.600$, for L3–L4 and L4–L5 levels, respectively).

Conclusion: This study suggests prone positioning may increase global lumbar lordosis, without changing the position of other major anatomical structures. The exiting nerve root positioning can be estimated in relation to foraminal height. These finding may help optimizing planning and minimizing iatrogenic lesions.

Level of Evidence: 3.

Other and Special Categories

Keywords: magnetic resonance, prone, lumbar spine, endoscopy, interbody fusion, minimally invasive spine surgery

INTRODUCTION

Spine surgery is undergoing technological advancements, with a trend to use minimally invasive spine (MIS) techniques and endoscopic procedures and to extend their indications. In fact, several studies suggest that these techniques are associated with reduced soft tissue damage, blood loss, postoperative pain, hospital stay, and recovery time while maintaining efficacy and safety (when compared to conventional open surgery). However, MIS and

endoscopic techniques have unique complications related to their steep learning curve and commonly performed technical variations.^{1–6} Therefore, to minimize the risk of such complications, surgeons need to have deep knowledge of spine anatomy. In fact, the upsurge of MIS and endoscopic procedures has contributed to a renewed interest in spine anatomy.^{7–9} Moreover, as techniques and approaches become more structured and tailored, preoperative planning becomes increasingly important in preventing unanticipated complications and optimizing outcomes.^{10–12} For

instance, given that positioning variations may potentially interfere with the location and morphological trends of anatomic structures, it is of utmost importance to study and understand these variations.

For lumbar disease, magnetic resonance imaging (MRI) is among the most widely used and valuable imaging techniques. Generally, it is performed in a supine/dorsal decubitus position as opposed to prone/ventral decubitus, the most frequently used surgical positioning. Although it has been used for the diagnosis of tethered cord syndrome, prone MRI is rarely used as a diagnostic tool in degenerative cases.^{13,14} Previous spinal MRI-based studies on the prone position were mostly performed in small samples, and recent works have tried to evaluate its utility in estimating lumbar nerve root and ganglion position, with variable results.¹⁵⁻¹⁷

As the impact of intraoperative prone positioning on lumbar spine anatomy remains unknown, prone MRI studies may provide new data and increase accuracy for spinal procedures. The aim of the present study is to describe lumbar morphology, nerve roots and related structures positioning in the prone position and to find potential relevant changes when compared with the conventional supine position in patients with lumbar symptoms. The secondary aim is to help define safe working zones for MIS and endoscopic procedures to reduce the risk of iatrogenic lesions.

METHODS

Study Design, Setting, and Participants

This was an observational cross-sectional study performed in a single center (Unidade Local de Saúde de São João, Porto; the largest tertiary hospital in Northern Portugal). Approval was granted by the Ethics Committee of Centro Hospitalar Universitário de São João/Faculdade de Medicina da Universidade do Porto, in May 2023 (CE 73/2023). The study was conducted between July and December 2023. We included a consecutive sample of patients who attended the outpatient clinics of our center, met eligibility criteria and provided informed consent.

Participants were included if they were adults (aged ≥ 18 years) with persistent low back and/or radicular pain that was unresponsive to conservative treatment and if they were willing to participate and able to understand the study protocol.

Exclusion criteria included age < 18 years; pregnancy; previously known spine deformity (such as high-grade spondylolisthesis, scoliosis, or fracture); previous abdominal, retroperitoneal, or spine surgery; and/or

contraindication for MRI (such as the presence of ferromagnetic material).

Variables and Data Sources

Clinical and demographic data were collected from all patients. In particular, we collected data on the following variables during medical consultation: age, gender, height, weight and spine-related symptoms. Additionally, we collected information from MRI to compare results obtained in supine and prone positions.

MRI Acquisition and Patient Positioning

The MRI protocol was defined between orthopedic surgeons and neuroradiologists. Patients were scanned in a 3 Tesla MRI (Magnetom TrioTrim, Siemens Healthcare) equipped with multichannel body antennas. A 2D sagittal plane T2-weighted turbo-spin-echo sequence (TR/TE = 3750/84 ms, flip angle = 135, matrix = 384 \times 288, echo train length = 19, and slice thickness = 3 mm), along with an axial 2D T2-weighted turbo-spin-echo sequence (TR/TE = 5930/117 ms, flip angle = 130, matrix = 384 \times 250, echo train length = 22, and slice thickness = 3 mm) was acquired in supine position and then repeated in prone position. During the latter, support pillows were placed between the table and the patient's chest and pelvis (Figure 1) to reduce motion artifacts from breathing. Additionally, clinical 2D T1W and short-tau inversion recovery acquisitions were obtained but were not analyzed in this work.

Imaging Analysis

Two researchers independently conducted all measurements described below, using the Sectra IDS7 software. Any significant discrepancies were solved by a third supervising author.

Imaging analysis included median sagittal plane, bilateral sagittal plane (midpedicular), and axial plane (mid-intervertebral disc [IVD]) variables, as described below:

- Median sagittal plane analysis and measurements
 - IVD degeneration and listhesis grading (as classified by Pfirrmann and Meyerding classifications, respectively).
 - Lumbar lordosis (LL): angle ($^{\circ}$) between the upper endplate of L1 and the upper endplate of S1 vertebrae (Figure 2).
 - Lower lumbar lordosis (LLL): angle ($^{\circ}$) between the upper endplate of L4 and the upper endplate of S1 vertebrae (Figure 2).

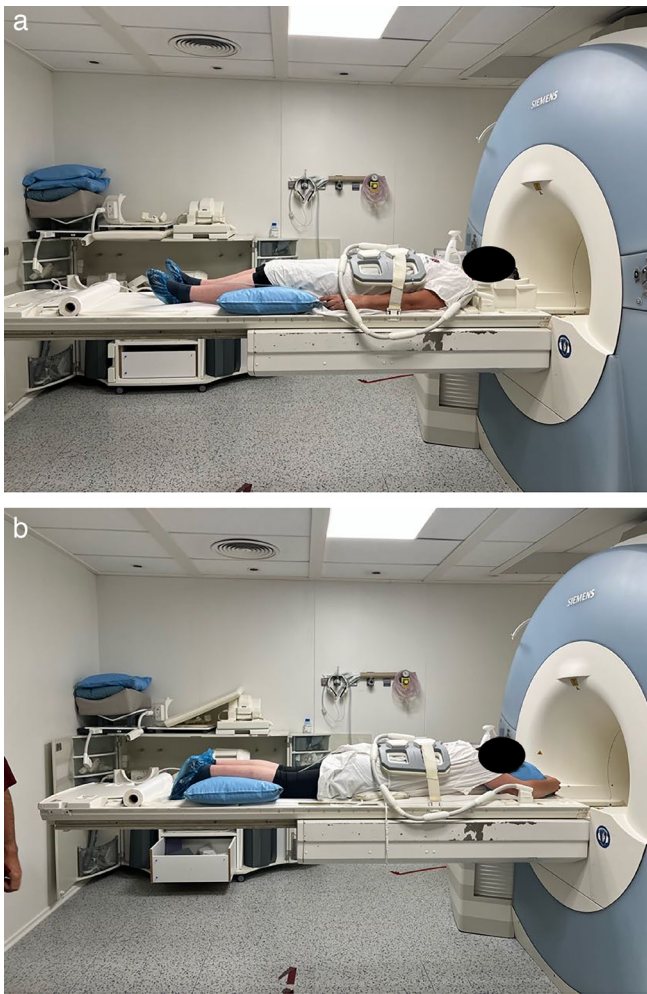


Figure 1. Patient positioning for supine (a) and prone (b) magnetic resonance imaging.



Figure 3. Anterior (a), middle (m), and posterior (p) intervertebral disc height.

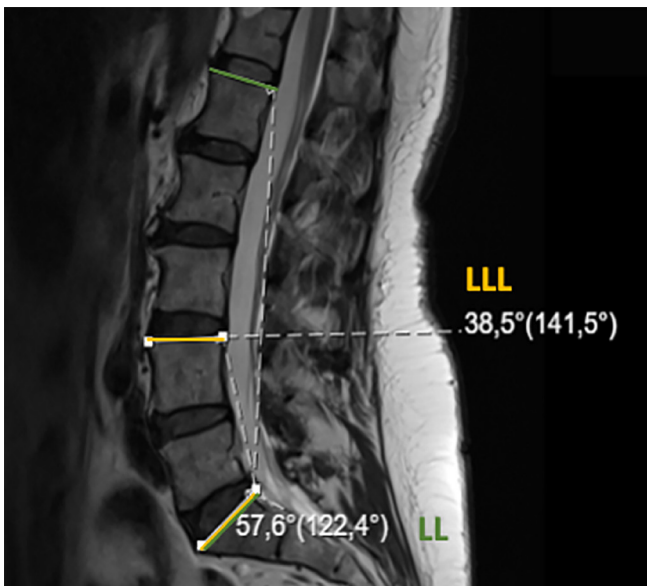


Figure 2. Lumbar lordosis (LL; green) and lower lumbar lordosis (LLL; yellow).

- Anterior, middle, and posterior IVD height for L3 to L4, L4 to L5, and L5 to S1 levels: distance (millimeters) between the upper and lower endplates of each segment at the anterior, middle, and posterior disc locations (Figure 3).
- Bilateral sagittal plane (midpedicular) analysis and measurements:
 - Foraminal height (FH) for L3 to L4, L4 to L5, and L5 to S1 levels: longitudinal distance (millimeters) between the inferior pedicle wall of the upper level and the superior pedicle wall of the level below (Figure 4).
 - Root-to-pedicle (RtP) distance for L3 to L4, L4 to L5, and L5 to S1 levels: longitudinal distance (millimeters) between the inferior border of the

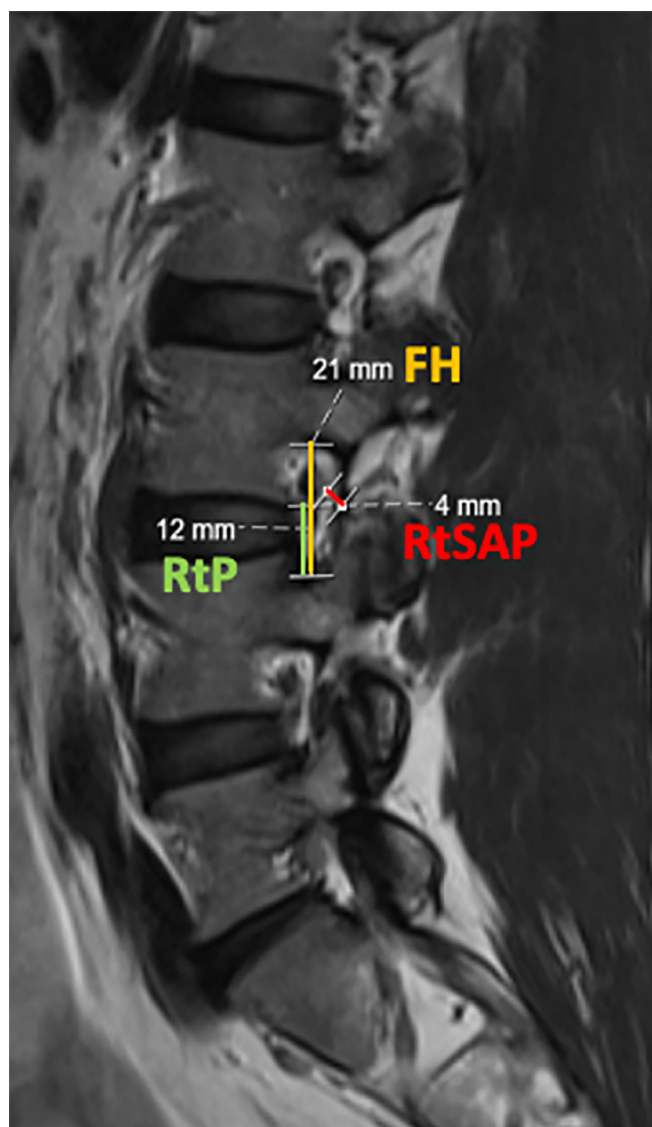


Figure 4. Foraminal height (FH), root to pedicle (RtP), and root to superior articular process (RtSAP) distances.

emerging nerve root and the superior pedicle wall of the level below (Figure 4).

- Root-to-superior articular process (RtSAP) distance for L3 to L4, L4 to L5, and L5 to S1 levels: distance (millimeters) from the emerging nerve root to the tip of the superior articular process (Figure 4).
- Axial plane (mid-IVD) analysis and measurements:
 - Lumbar stenosis grading (according to the Schizas classification).
 - Safe corridor for L3 to L4 and L4 to L5 levels: measurement of the left corridor (mm) for lateral lumbar interbody fusion (LLIF) at the mid-IVD position (Figure 5).
 - Description of signs of segmental instability.

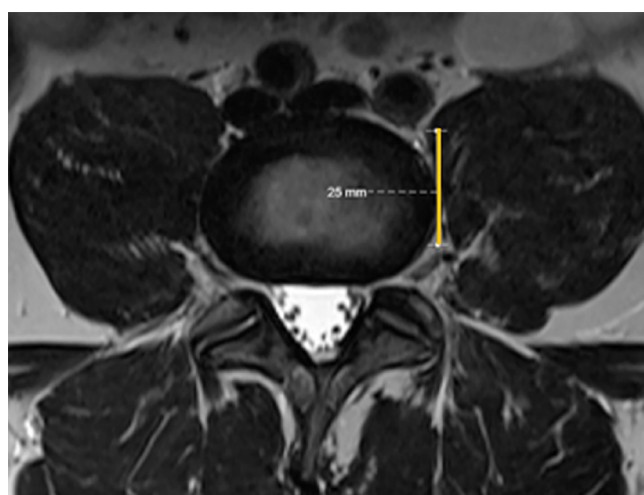


Figure 5. Left lateral safe corridor (yellow line) for lateral lumbar interbody fusion approach.

Statistical Analysis

Continuous variables were described using means \pm SDs, while categorical variables were described using absolute and relative frequencies. We performed a paired Student *t* test (for continuous variables) or χ^2 /Fisher's exact test (for categorical variables) to evaluate each parameter between supine and prone positions. In addition, to evaluate interobserver reliability, we computed intraclass correlation coefficients (ICC) and their 95% confidence intervals. ICC estimates were calculated based on a mean rating ($k = 2$), consistency agreement, and 2-way random-effects model.¹⁸

Statistical analysis was performed using SPSS version 27.0 (IBM Corp., USA), and *P* values less than 0.05 were considered statistically significant.

RESULTS

Fifty patients were included. Four cases were subsequently excluded due to claustrophobia ($n = 2$) or imaging artifacts precluding adequate analysis ($n = 2$). Therefore, a total of 46 cases (28 female patients; 61%) were analyzed. Participants' mean age was 50.3 ± 9.4 years, and the most common complaints were lumbar pain ($n = 19$), radicular pain ($n = 7$), or both ($n = 20$).

Median Sagittal Plane Analysis and Measurements

Based on supine MRI analysis, all patients presented some degree of lumbar IVD degeneration and disc height loss (Pfirrmann grading III–V) was evident in 37%, 59%, and 63% of patients for L3 to L4, L4 to L5, and L5 to S1 levels, respectively. In prone MRI

Table 1. Lumbar lordosis and IVDh comparison from supine to prone.

Variable	Supine Position, Mean (SD)	Prone Position, Mean (SD)	Paired Difference (95% CI)	P
Lumbar lordosis (°)	49.3 (9.3)	52.1 (10.0)	-2.8 (-4.7, -0.9)	0.005
Lower lumbar lordosis (°)	36.9 (6.0)	36.4 (6.5)	0.5 (-0.7, 1.7)	0.404
L3-L4 anterior IVDh (mm)	9.3 (1.6)	9.7 (1.5)	-0.3 (-0.6, -0.1)	0.015
L3-L4 middle IVDh (mm)	10.2 (2.1)	10.4 (1.9)	-0.2 (-0.5, 0.0)	0.101
L3-L4 posterior IVDh (mm)	6.5 (1.5)	6.5 (1.5)	0.0 (-0.3, 0.2)	0.800
L4-L5 anterior IVDh (mm)	10.2 (2.2)	10.4 (2.0)	-0.2 (-0.5, 0.1)	0.142
L4-L5 middle IVDh (mm)	10.2 (2.3)	10.2 (2.1)	0.0 (-0.2, 0.0)	0.914
L4-L5 posterior IVDh (mm)	6.0 (1.5)	6.3 (1.5)	-0.3 (-0.6, -0.1]	0.353
L5-S1 anterior IVDh (mm)	11.7 (2.9)	11.7 (2.7)	0.0 (-0.4, 0.4)	1.000
L5-S1 middle IVDh (mm)	9.2 (2.7)	9.2 (2.9)	0.0 (-0.3, 0.3)	0.876
L5-S1 posterior IVDh (mm)	5.1 (1.3)	5.4 (1.7)	-0.3 (-0.6, 0.0)	0.032

Abbreviations: CI, confidence interval; IVDh, intervertebral disc height.

analysis, results were similar, and statistically significant differences were not found.

Regardingolisthesis, grade I spondylolisthesis was identified in 14 supine MRI cases (L3-L4 level: $n = 2$; L4-L5 level: $n = 10$; L5-S1 level: $n = 2$). In prone MRI analysis, 4 additional cases were identified ($P = 0.001$).

Table 1 summarizes and compares LL, LLL, and IVD heights in both positions. A high degree of interobserver reliability was found between LL and LLL measurements, with an average LL ICC 0.962 (95% CI 0.910, 0.986) and average LLL ICC 0.921 (95% CI 0.857, 0.956); reliability for IVD heights was good, with average ICC always above 0.800. Mean LL was 49.3° in the supine compared to 52.1° in the prone position ($P = 0.005$), while mean LLL suffered no statistically significant variation (36.9° in supine vs 36.4° in the prone). Moreover, positional differences were

evident at L3 to L4 anterior IVD height (paired difference -0.3 mm, 95% CI -0.6, -0.1; $P = 0.015$) and L5 to S1 posterior IVD height (paired difference -0.3 mm, 95% CI -0.6, 0.0; $P = 0.032$), with higher values in the prone position.

Bilateral Sagittal Plane (Midpedicular) Analysis and Measurements

Measurements of both left and right FH at L3 to L4, L4 to L5, and L5 to S1 levels, longitudinal RtP distance, and RtSAP distances are depicted in Table 2. Average ICC ranged from 0.776 to 0.912. No statistically significant differences were found, except for left L5 to S1 FH (paired difference -0.8 mm, 95% CI -1.3, -0.3; $P = 0.001$), right L4 to L5 FH (paired difference 0.4 mm, 95% CI 0.0, 0.9; $P = 0.039$), right L4 to L5 (paired

Table 2. Foraminal height, root-to-pedicle, and RtSAP distances comparison from supine to prone.

Variable	Supine Position, Mean (SD)	Prone Position, Mean (SD)	Paired Difference (95% CI)	P
Left Foraminal Height				
L3-L4	19.7 (2.2)	19.4 (2.0)	0.3 (-0.1, 0.7)	0.172
L4-L5	18.2 (1.7)	18.2 (1.7)	0.0 (-0.4, 0.3)	0.859
L5-S1	15.6 (2.0)	16.4 (1.7)	-0.8 (-1.3, -0.3)	0.001
Right Foraminal Height				
L3-L4	19.5 (1.9)	19.2 (2.1)	0.4 (-0.1, 0.8)	0.086
L4-L5	18.3 (1.6)	17.8 (2.0)	0.4 (0.0, 0.9)	0.039
L5-S1	16.9 (2.0)	16.5 (2.1)	0.4 (-0.1, 0.8)	0.093
Left Root-to-Pedicle				
L3-L4	8.2 (1.8)	8.6 (2.1)	-0.3 (-0.8, 0.1)	0.166
L4-L5	8.3 (1.8)	8.1 (1.7)	0.2 (-0.3, 0.6)	0.442
L5-S1	7.3 (1.9)	7.4 (1.5)	-0.1 (-0.6, 0.3)	0.519
Right Root-to-Pedicle				
L3-L4	9.4 (1.8)	8.8 (1.6)	0.6 (0.0, 1.2)	0.065
L4-L5	9.0 (1.6)	8.5 (1.8)	0.5 (0.0, 1.0)	0.055
L5-S1	8.3 (1.3)	8.2 (2.1)	0.1 (-0.5, 0.6)	0.811
Left RtSAP				
L3-L4	2.3 (1.1)	2.9 (0.9)	-0.5 (-0.8, -0.2)	0.052
L4-L5	2.6 (1.1)	2.5 (0.7)	0.1 (-0.2, 0.4)	0.598
L5-S1	2.5 (1.2)	2.7 (0.8)	-0.1 (-0.5, 0.2)	0.405
Right RtSAP				
L3-L4	2.3 (1.1)	2.4 (0.9)	-0.1 (-0.4, 0.2)	0.434
L4-L5	2.1 (1.0)	2.4 (0.7)	-0.4 (-0.6, -0.1)	0.003
L5-S1	2.3 (1.1)	2.6 (0.8)	-0.3 (-0.5, 0.0)	0.049

Abbreviation: RtSAP, root-to-superior articular process.

Table 3. Relationship between root-to-pedicle and foraminal height.

Variable	Supine Position, Ratio (SD)	Prone Position, Ratio (SD)	Paired Difference (95% CI)	P
Left L3–L4	0.42 (0.81)	0.44 (0.90)	–0.02 (–0.05, 0.00)	0.069
Left L4–L5	0.45 (0.81)	0.45 (0.75)	0.00 (–0.01, 0.03)	0.412
Left L5–S1	0.47 (0.11)	0.45 (0.79)	0.01 (–0.01, 0.04)	0.311
Right L3–L4	0.48 (0.78)	0.46 (0.68)	0.02 (–0.01, 0.05)	0.203
Right L4–L5	0.45 (0.81)	0.45 (0.75)	0.01 (–0.01, 0.03)	0.412
Right L5–S1	0.49 (0.77)	0.49 (0.95)	0.00 (–0.03, 0.03)	0.984

difference –0.4 mm, 95% CI –0.6, –0.1; *P* = 0.003), and right L5 to S1 (paired difference –0.3 mm, 95% CI –0.5, 0.0; *P* = 0.049) RtSAP distances.

To estimate the longitudinal position of the root within the foramen, the relationship between FH and RtP was established, as defined by RtP/FH. Results are presented in Table 3, and no statistically significant differences were found between supine and prone positions. The exiting nerve root was found between 42% and 49% of the FH, as measured from the upper border of the lower pedicle.

Axial Plane (Mid-IVD) Analysis and Measurements

The lateral lumbar working corridor (see Table 4) suffered no statistically significant size variation from the supine to prone position for both L3 to L4 and L4 to L5 levels (*P* = 0.196 and *P* = 0.600, respectively; with average ICC ranging from 0.799 to 0.937). Globally, the working window for LLIF was significantly narrower at the L4 to L5 level (*P* < 0.001 for both supine and prone positions when compared with L3 to L4 space), potentially increasing the risk of complications when performing a prone LLIF at this level.

Additional analysis of axial T2-weighted images revealed dispersed facet joint fluid signal changes, suggestive of dynamic lumbar spine instability (Figure 6).

DISCUSSION

This study aimed to assess differences in lumbar morphology and nerve root positioning between supine and prone decubitus, using a 3 Tesla MRI. To the best of our knowledge, this is one of the most extensive quantitative analysis of lumbar positional changes using MRI.

Median Sagittal Plane Analysis and Measurements

The dynamic nature of the spine and its contribution to symptomatic degenerative disease is evident in this study, as prone MRI analysis revealed additional cases of grade I spondylolisthesis (*P* = 0.001) compared to supine imaging, suggestive of lumbar instability. Positional changes in lumbar parameters have been widely described, mainly using simple radiography.^{19–21} However, quantitative MRI analysis of LL and IVD height variation from supine to prone is poorly described. Similar to results from Amaral et al¹⁵ and Yingsakmongkol et al,¹⁷ the current study suggests that prone position may improve global LL, optimizing preoperative conditions in lumbar fusion procedures, where LL correction and sagittal balance reestablishment are paramount features.

Bilateral Sagittal Plane (Midpedicular) Analysis and Measurements

Changes in foraminal measures have become clear while studying cervical and lumbar spine motion, again revealing the dynamic range of effects achievable in the spine.^{22–24} However, in this study, no consistent changes were found for FH, RtP, or RtSAP distances. We hypothesize that their magnitude might be minimal and consequently could not be detected, as the minimal difference using this software is 1 mm.

Moreover, RtP/FH relation showed that the exiting nerve root can be found between 42% and 49% of the FH. We believe that foraminal ligaments (FLs) might play a role in this finding. Elaborating on this theory, previous anatomical works have demonstrated that FLs connect spinal nerves with the bordering structures such as lumbar vertebral bodies, IVD, ligamentum flavum, articular processes and facet joint capsules.^{25–27}

Table 4. Lateral lumbar working corridor.

Variable	Supine Position, Mean (SD)	Prone Position, Mean (SD)	Paired Difference (95% CI)	P
L3–L4 Corridor	21.2 (5.3)	20.8 (5.2)	0.4 (–0.2, 1.1)	0.196
L4–L5 Corridor	15.9 (4.6)	15.7 (4.2)	0.2 (–0.6, 1.0)	0.600

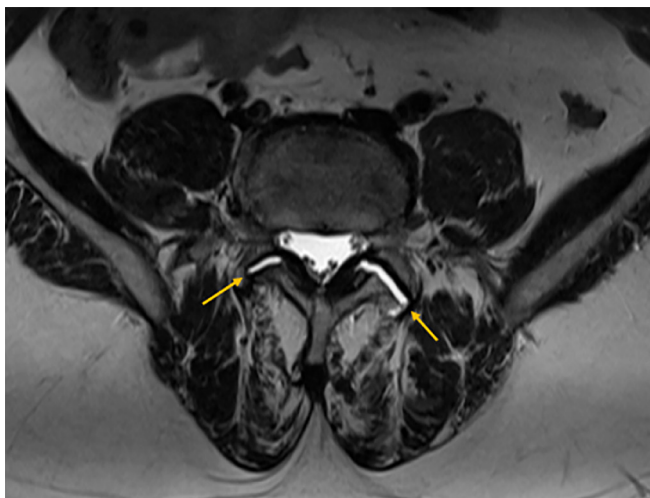


Figure 6. Disperse facet joint fluid signal changes (arrow), suggestive of dynamic lumbar spine instability.

Therefore, FLs may stabilize the nerve root within the foramen or, in pathological cases, contribute to its compression. Interestingly, Jack et al performed cadaveric dissections in the cervical spine and demonstrated that cutting the FLs results in the detethering of the nerve roots, indirectly suggesting their role as “stabilizers”.²⁸

Axial Plane (Mid-IVD) Analysis and Measurements

Measurement of the left retroperitoneal lateral corridor for LLIF at both L3 to L4 and L4 to L5 levels revealed no significant size variation from the supine to the prone position. This is supported by the work of Yingsakmongkol et al¹⁷ who found no major differences in lumbar nerve roots, psoas muscle morphology and great vessels position between supine and prone positions. On the contrary, Amaral et al¹⁵ and Munim et al²⁹ suggested posterior psoas muscle retraction in the prone position.

Globally, the working window for instrumentation was significantly narrower at L4 to L5 than at L3 to L4 level, likely increasing the risk of complications at the lower level while performing a prone LLIF, as corroborated by the cadaveric work from Guérin et al.³⁰

Moreover, in a descriptive analysis of axial T2-weighted images, changes in facet joints fluid signals were found in some cases, suggesting dynamic lumbar spine instability, which may contribute to mechanical and/or neurological symptoms.

Limitations and Strengths

Our main limitation concerns the relatively small number of patients included in this pilot study. In

addition, patients with previous surgeries or existing metallic hardware were not assessed, which may limit the interpretation of these results to this subgroup that may have a stiffer and more degenerated spine with fibrotic changes. Moreover, the degree of degenerative changes ranged widely among participants. A third issue relates to patient positioning to minimize imaging artifacts in prone MRI, and 2 support pillows were used; the lower one, placed over the abdomen/pelvic area, may have influenced positional changes in lumbar parameters, as IVD height suggests an inflection point approximately at the L4 to L5 level. Therefore, LL might be even higher, and LLL may increase in the prone position.

The present study also has some strengths. First, it is one of the most extensive quantitative analysis of lumbar positional changes using MRI. Second, ICC revealed good to excellent interobserver reliability among measurements. Third, this study may have some implications for clinical practice, such as helping to estimate the lumbar nerve root position within the foramen or providing useful insights of pain generators in patients with minimal changes in supine images, such as signs of segmental instability.

CONCLUSION

This study shows that the prone position increased global LL, with no other major anatomical variations between supine and prone imaging. Consistently, the exiting nerve root was found around half of the FH. Comparing supine and prone MRI may reveal additional instability levels that may contribute to the mechanical or neurological symptoms.

REFERENCES

1. Chen K-T, Kim J-S, Huang AP-H, Lin MH-C, Chen C-M. Current indications for spinal endoscopic surgery and potential for future expansion. *Neurospine*. 2023;20(1):33–42. doi:10.14245/ns.2346190.095
2. Kimchi G, Orlev A, Hadanny A, Knoller N, Harel R. Minimally invasive spine surgery: the learning curve of a single surgeon. *Global Spine J*. 2020;10(8):1022–1026. doi:10.1177/2192568219880872
3. Wang TY, Wang MY. Advances and challenges in minimally invasive spine surgery. *J Clin Med*. 2024;13(11):3329:11. doi:10.3390/jcm13113329
4. Relvas-Silva M, Pinto BS, Sousa A, Loureiro M, Pinho AR, Pereira P. Is endoscopic technique an effective and safe alternative for lumbar interbody fusion? A systematic review and meta-analysis. *EFORT Open Rev*. 2024;9(6):536–555. doi:10.1530/EOR-23-0167
5. Ozgur BM, Aryan HE, Pimenta L, Taylor WR. Extreme lateral interbody fusion (XLIF): a novel surgical technique for anterior lumbar interbody fusion. *Spine J*. 2006;6(4):435–443. doi:10.1016/j.spinee.2005.08.012

6. Casal Grau R, Sánchez Benitez de Soto FJ, Barhouse P, et al. Endoscopic lateral lumbar interbody fusion: technical note and case series. *Int J Spine Surg.* 2024;18(1):101–109. doi:10.14444/8572
7. Sun H, Fan C, Zhou X, et al. Anatomical study of the relationship between the lumbar intervertebral disc, nerves, and psoas major. *Clin Anat.* 2025;38(1):20–28. doi:10.1002/ca.24177
8. Uchikado H, Nishimura Y, Hattori G, Ohara Y. Micro-anatomical structures of the lumbar intervertebral foramen for full-endoscopic spine surgery: review of the literatures. *J Spine Surg.* 2020;6(2):405–414. doi:10.21037/jss.2019.10.07
9. Uribe JS, Arredondo N, Dakwar E, Vale FL. Defining the safe working zones using the minimally invasive lateral retroperitoneal transpsoas approach: an anatomical study. *J Neurosurg Spine.* 2010;13(2):260–266. doi:10.3171/2010.3.SPINE09766
10. Fujita M, Kawano H, Kitagawa T, et al. Preoperative design for the posterolateral approach in full-endoscopic spine surgery for the treatment of L5/S1 lumbar disc herniation. *Neurospine.* 2019;16(1):105–112. doi:10.14245/ns.1836316.158
11. Lee JU, Park KJ, Kim KH, Choi MK, Lee YH, Kim D-H. What is the ideal entry point for transforaminal endoscopic lumbar discectomy? *J Korean Neurosurg Soc.* 2020;63(5):614–622. doi:10.3340/jkns.2020.0050
12. Telfeian AE, Wagner R. Transforaminal endoscopic thoracic discectomy: surgical technique. *J Spine Surg.* 2023;9(2):166–175. doi:10.21037/jss-22-109
13. Aoun SG, El Ahmadieh TY, Vance AZ, Neeley O, Morrill KC. The use of prone magnetic resonance imaging to rule out tethered cord in patients with structural spine anomalies: a diagnostic technical note for surgical decision-making. *Cureus.* 2019;11(3):e4221. doi:10.7759/cureus.4221
14. Stamates MM, Frim DM, Yang CW, Katzman GL, Ali S. Magnetic resonance imaging in the prone position and the diagnosis of tethered spinal cord. *J Neurosurg Pediatr.* 2018;21(1):4–10. doi:10.3171/2017.3.PEDS16596
15. Amaral R, Daher MT, Pratali R, et al. The effect of patient position on psoas morphology and in lumbar lordosis. *World Neurosurg.* 2021;153:e131–e140. doi:10.1016/j.wneu.2021.06.067
16. Avellanal M, Ferreira A, Riquelme I, Boezaart AP, Prats-Galino A, Reina MA. Prone position MRI of the lumbar spine in patients with low back pain and/or radiculopathy refractory to treatment. *Pain Physician.* 2022;25(5):409–418.
17. Yingsakmongkol W, Poriswanich K, Kotheeranurak V, Numkarunaranrote N, Limthongkul W, Singhatanadgige W. How prone position affects the anatomy of lumbar nerve roots and psoas morphology for prone transpsoas lumbar interbody fusion. *World Neurosurg.* 2022;160:e628–e635. doi:10.1016/j.wneu.2022.01.104
18. Koo TK, Li MY. A guideline of selecting and reporting intraclass correlation coefficients for reliability research. *J Chiropr Med.* 2016;15(2):155–163. doi:10.1016/j.jcm.2016.02.012
19. Mills ES, Wang JC, Richardson MK, et al. The change in lumbar lordosis from the standing to the lateral position: implications for lateral interbody fusion. *Eur Spine J.* 2025;34(1):148–155. doi:10.1007/s00586-024-08493-2
20. Yasuda T, Hasegawa T, Yamato Y, et al. Effect of position on lumbar lordosis in patients with adult spinal deformity. *J Neurosurg Spine.* 2018;29(5):530–534. doi:10.3171/2018.3.SPINE1879
21. Arab AM, Haghight A, Amiri Z, Khosravi F. Lumbar lordosis in prone position and prone hip extension test: comparison between subjects with and without low back pain. *Chiropr Man Therap.* 2017;25:8. doi:10.1186/s12998-017-0139-x
22. Inufusa A, An HS, Lim T-H, Hasegawa T, Haughton VM, Nowicki BH. Anatomic changes of the spinal canal and intervertebral foramen associated with flexion-extension movement. *Spine (Phila Pa 1986).* 1996;21(21):2412–2420. doi:10.1097/00007632-199611010-00002
23. Liu M-Y, Wang H-B, Liu S-W, Zhang G-P, Liu J-G, Yang C. Dimensional changes of lumbar intervertebral foramen in direct anterior approach-specific hyperextension supine position. *Orthop Surg.* 2020;12(4):1173–1181. doi:10.1111/os.12728
24. Hutchins J, Lagerstrand K, Stävliid E, et al. MRI evaluation of foraminal changes in the cervical spine with assistance of a novel compression device. *Sci Rep.* 2023;13(1):11508. doi:10.1038/s41598-023-38401-5
25. Zhong E, Fan C, Li Q, Zhao Q. A comparative study of the anatomy and MRI images of the lumbar foraminal ligaments at the L1-L5 levels. *Surg Radiol Anat.* 2023;45(12):1535–1543. doi:10.1007/s00276-023-03251-3
26. Henkelmann J, Wiersbicki D, Steinke H, Denecke T, Heyde C-E, Voelker A. In vivo detection of the lumbar intraforaminal ligaments by MRI. *Eur Spine J.* 2022;31(4):882–888. doi:10.1007/s00586-022-07153-7
27. Wiersbicki D, Völker A, Heyde C-E, Steinke H. Ligament compartments and their relation to the passing spinal nerves are detectable with MRI inside the lumbar neural foramina. *Eur Spine J.* 2019;28(8):1811–1820. doi:10.1007/s00586-019-06024-y
28. Jack AS, Osburn BR, Tymchak ZA, et al. Foraminal ligaments tether upper cervical nerve roots: a potential cause of postoperative C5 palsy. *J Brachial Plex Peripher Nerve Inj.* 2020;15(1):e9–e15. doi:10.1055/s-0040-1712982
29. Munim MA, Nolte MT, Federico VP, et al. The effect of intraoperative prone position on psoas morphology and great vessel anatomy: consequences for prone lateral approach to the lumbar spine. *World Neurosurg.* 2024;181:e578–e588. doi:10.1016/j.wneu.2023.10.096
30. Guérin P, Obeid I, Gille O, et al. Safe working zones using the minimally invasive lateral retroperitoneal transpsoas approach: a morphometric study. *Surg Radiol Anat.* 2011;33(8):665–671. doi:10.1007/s00276-011-0798-6

Funding: This study was funded by the Project SSIn - Spine Surgery Innovation (Code: 79701) - Faculty of Medicine of University of Porto.

Declaration of Conflicting Interests: The authors report no conflicts of interest in this work.

Patient Consent: Informed consent was obtained from all individual participants included in the study.

Ethics Approval: This study was performed in line with the principles of the Declaration of Helsinki. Approval was granted by the Ethics Committee of Centro Hospitalar Universitário de São João/Faculdade de Medicina da Universidade do Porto, in May, 2023 (CE 73/2023).

Author Contributions: Study conception and design: all authors. Methodology: Miguel Silva, André Pinho, Maria Dulce Madeira, and Pedro Alberto Pereira.

Material preparation and data collection and analysis: Miguel Silva, Daniel Dias, José Sousa, Vitorino Veludo, and Bernardo Sousa Pinto. Writing—original draft preparation: Miguel Silva, José Sousa, and Bernardo Sousa Pinto. Writing—review and editing: André Pinho, Miguel Loureiro, António Sousa, António Serdoura, José Fonseca, and Pedro Alberto Pereira. Supervision: Vitorino Veludo, Maria Dulce Madeira, and Pedro Alberto Pereira.

Corresponding Author: Miguel Relvas-Silva, Department of Surgery and Physiology, Faculty of Medicine, University of Porto, Alameda Professor Hernâni Monteiro, 4200-319 Porto, Portugal; mrelvas.silva@gmail.com

Copyright © 2025 ISASS. The IJSS is an open access journal following the Creative Commons Licensing Agreement CC BY-NC-ND. To learn more or order reprints, visit <http://ijssurgery.com>.